

# Solvent-induced framework-interpenetration isomers and tuning of porosity of In-MOFs for efficient proton conduction and fluorescence sensing

## EXPERIMENTAL SECTION

### Materials and instrumentation

All reagents were obtained commercially and can be used directly. Fourier transform infrared spectra (FT-IR) were measured on KBr pellets with a Perkin Elmer Spectrum Two spectrometer (400-4000  $\text{cm}^{-1}$ ) at 298 K. Powder X-ray diffraction (PXRD) data were collected over the  $2\theta$  range of 5–50° using a Bruker D8 ADVANCE powder X-ray diffractometer with Cu  $K\alpha$  radiation ( $\lambda=1.5418 \text{ \AA}$ ) at room temperature. Thermal gravimetric analysis (TGA) was performed on Perkin-Elmer TGA-7 thermogravimetric analyzer in a nitrogen atmosphere from room temperature to 800°C with a heating rate of 5 °C/min. The fluorescence spectra of the compound **2** in the solid state and their samples in H<sub>2</sub>O was measured on a Techcomp FL-970 spectrophotometer equipped with a Xe lamp and a quartz carrier. The UV–vis absorption spectra were recorded on a SHIMADZU UV-2600 spectrometer. The LUMO–HOMO energy levels were calculated by the density functional theory (DFT) method at the B3LYP/6-31G\*\* level in the Gaussian 09 program package.

### Conductometric Measurements

Electrical conductivity of compounds was test by impedance spectroscopy on the CHI 660E with an input voltage of 200 mV over a frequency domain of 1 Hz-1 MHz. Prior to making measurements, the as-synthesized samples were pressed into pellets of 13.0 mm diameter and ~1 mm thickness at a pressure of 6 MPa for 2 min. All the samples were completely hydrated in the corresponding %RH atmosphere for 24 h prior to the test. The AC impedance spectra were obtained in the temperatures range of 303–373 K and the relative humidity's range of 58–98%. The proton conductivity ( $\sigma$ ) was calculated utilizing the following equation (1), where  $\sigma$  = proton conductivity

( $S \cdot \text{cm}^{-1}$ ),  $L$  = thickness of the tablet (cm),  $S$  = surface area of the tablet ( $\text{cm}^2$ ), and  $R$  = resistance ( $\Omega$ ).

$$\sigma = L/SR \quad (1)$$

The  $E_a$  value was calculated from the Arrhenius equation

$$\sigma T = \sigma_0 \exp\left(-E_a/k_B T\right) \quad (2)$$

where  $\sigma$  is the proton conductivity,  $\sigma_0$  is the preexponential factor,  $k_B$  is the Boltzmann constant, and  $T$  is the temperature.

### X-ray crystallography

Single-crystal X-ray diffraction data collection was collected on a XtaLAB Synergy-DS single crystal diffractometer, using graphite-monochromated Cu- $k\alpha$  radiation ( $\lambda = 1.54184 \text{ \AA}$ ) by using the  $\omega$ - $2\theta$  scan mode at temperature (110 K). The structures were solved by direct methods using SHELXL in conjunction with the OLEX2 graphical user interface. Topology information for compounds were calculated using TOPOS 5.4.

Even the low temperature data set obtained at about 110K for the compounds reveals highly disordered solvents within the lattice interstices. The diffraction data were treated by the mask routine of Olex2 (similar to PLATON/SQUEEZE). Commonly, it is a feasible way to assign the diffuse solvent according to the electrons in the void as reported in ref.[1-2]

Mask routine of Olex2 analyses estimate the electron count to be 380 within  $1953 \text{ \AA}^3$  void per cell for **1**, 596 within  $2498 \text{ \AA}^3$  void per cell for **2**. The TENTATIVE assignment of the solvents are described in detail as below.

#### (1) Solvents assignment in **1**.

The structure refinement of **1** with space group P4/nbm and sixteen formula units in one cell. The residual electron density was treated as diffuse contributions using the mask routine of Olex2 and located a series of voids with 380 electrons per cell, it might be possible that the formula unit includes 16  $(\text{CH}_3)_2\text{NH}_2$  (432 e).

#### (2) Solvents assignment in **2**.

The structure refinement of **2** with space group I-42d and sixteen formula units in one

cell. The residual electron density was treated as diffuse contributions using the mask routine of Olex2 and located a series of voids with 596 electrons per cell, it might be possible that the formula unit includes 16  $(\text{CH}_3)_2\text{NH}_2$  (432 e) and 16  $\text{H}_2\text{O}$  (160 e).

#### Luminescence Sensing Experiments.

To investigate the potential ability of compound **2** for fluorescence detection, a 2 mg portion of a ground samples of **2** added to 4 mL  $\text{H}_2\text{O}$  solutions of the different antibiotics (1 mmol/L) were respectively ultrasonicated for 30 min to form stable emulsions, and the corresponding luminescence spectra were measured. To study the selectivity and the detection capability of the sample for the different antibiotics, the titration experiments of **2** were conducted.

Table S1 Crystallographic data and structure refinement results for compounds **1-2**

Identification code	Compound 1	Compound 2
Empirical formula	C <sub>14</sub> H <sub>6</sub> InO <sub>8</sub>	C <sub>14</sub> H <sub>6</sub> InO <sub>8</sub>
Formula weight	417.01	411.02
Temperature/K	99.99(10)	100.00(10)
Crystal system	tetragonal	tetragonal
Space group	<i>P4/nbm</i>	<i>I-4<sub>2</sub>d</i>
<i>a</i> /Å	22.28670(10)	15.7171(3)
<i>b</i> /Å	22.28670 (10)	15.7171(3)
<i>c</i> /Å	8.55500(10)	30.1191(15)
$\alpha$ /°	90	90
$\beta$ /°	90	90
$\gamma$ /°	90	90
Volume/Å <sup>3</sup>	4249.24(6)	7440.2(5)
Z	8	16
$\rho_{\text{calc}}$ g/cm <sup>3</sup>	1.304	1.468
$\mu$ /mm <sup>-1</sup>	9.168	10.471
<i>F</i> (000)	1624.0	3153.0
Independent reflections	2312 [ <i>R</i> <sub>int</sub> =0.0456, <i>R</i> <sub>sigma</sub> =0.0125]	3600 [ <i>R</i> <sub>int</sub> =0.0254, <i>R</i> <sub>sigma</sub> =0.0227]
Goodness-of-fit on <i>F</i> <sup>2</sup>	1.124	1.092
Final <i>R</i> indexes [ <i>I</i> ≥2σ( <i>I</i> )]	<i>R</i> <sub>1</sub> =0.0861, <i>wR</i> <sub>2</sub> =0.2785	<i>R</i> <sub>1</sub> =0.0413, <i>wR</i> <sub>2</sub> =0.1177
Final <i>R</i> indexes [all data]	<i>R</i> <sub>1</sub> =0.0920, <i>wR</i> <sub>2</sub> =0.2889	<i>R</i> <sub>1</sub> =0.0436, <i>wR</i> <sub>2</sub> =0.1197
Largest diff. peak/hole/eÅ <sup>-3</sup>	1.75/-0.74	0.98/-0.45
Flack parameter	/	-0.012(7)

Table S2 The synthesis conditions, the topological structure analysis, the solvent-accessible volume (%) and the degree of interpenetration of compounds **1-2**

No.	the solvent-accessible volume	synthesis conditions	Topological nodes and symbols	the degree of interpenetration
<b>1</b>	45.3% (1925.0 Å <sup>3</sup> out of the 4249.2 Å <sup>3</sup> unit cell volume)	130 °C, DMF(2 mL)/MeCN (2 mL), HNO <sub>3</sub> (100 μL)	dia, 6 <sup>6</sup>	4-fold interpenetrating framework
<b>2</b>	32.2% (2399.2 Å <sup>3</sup> out of the 7440.2 Å <sup>3</sup> unit cell volume)	130 °C, DEF(2 mL)/MeCN (1 mL), HNO <sub>3</sub> (100 μL)	New topology, {4 <sup>8</sup> .6 <sup>20</sup> }	self-interpenetrating framework

Table S3 Proton conductivities ( $\text{S}\cdot\text{cm}^{-1}$ ) for compound **1** at different RHs and various temperatures

	58% RH <sup>a</sup>	76% RH <sup>a</sup>	86% RH <sup>a</sup>	98% RH <sup>a</sup>
30°C <sup>b</sup>	$2.04\times 10^{-6}$	$2.13\times 10^{-5}$	$3.26\times 10^{-5}$	$1.72\times 10^{-4}$
40°C <sup>b</sup>	$9.99\times 10^{-6}$	$3.26\times 10^{-5}$	$5.12\times 10^{-5}$	$2.62\times 10^{-4}$
50°C <sup>b</sup>	$2.39\times 10^{-5}$	$5.45\times 10^{-5}$	$8.78\times 10^{-5}$	$3.85\times 10^{-4}$
60°C <sup>b</sup>	$6.34\times 10^{-5}$	$1.42\times 10^{-4}$	$2.03\times 10^{-4}$	$7.45\times 10^{-4}$
70°C <sup>b</sup>	$2.01\times 10^{-4}$	$3.14\times 10^{-4}$	$4.09\times 10^{-4}$	$1.14\times 10^{-3}$
80°C <sup>b</sup>	$3.64\times 10^{-4}$	$5.92\times 10^{-4}$	$7.80\times 10^{-4}$	$1.82\times 10^{-3}$
90°C <sup>b</sup>	$7.11\times 10^{-4}$	$1.79\times 10^{-3}$	$2.22\times 10^{-3}$	$2.77\times 10^{-3}$
100°C <sup>b</sup>	$1.09\times 10^{-3}$	$2.65\times 10^{-3}$	$2.88\times 10^{-3}$	$4.08\times 10^{-3}$

<sup>a</sup>Relative humidity. <sup>b</sup>Temperature

Table S4 Proton conductivities ( $\text{S}\cdot\text{cm}^{-1}$ ) for compound **2** at 98% RHs and various temperatures

	30°C <sup>b</sup>	40°C <sup>b</sup>	50°C <sup>b</sup>	60°C <sup>b</sup>	70°C <sup>b</sup>	80°C <sup>b</sup>	90°C <sup>b</sup>	100°C <sup>b</sup>
98% RH <sup>a</sup>	$3.43\times 10^{-5}$	$4.76\times 10^{-5}$	$8.27\times 10^{-5}$	$1.13\times 10^{-4}$	$1.66\times 10^{-4}$	$3.05\times 10^{-4}$	$4.76\times 10^{-4}$	$7.00\times 10^{-4}$

<sup>a</sup>Relative humidity. <sup>b</sup>Temperature

Table S5 Proton conductive MOFs and their proton conductivity

Materials	Proton conductivity ( $\text{S}\cdot\text{cm}^{-1}$ )	Condition	References <sup>a</sup>
$[\text{Mn}(\text{H}_2\text{BBT})_2(\text{H}_2\text{O})_2]_n$	$1.69\times 10^{-5}$	100°C, 98% RH	[3]
$[\text{Ce}_2(\text{HMIDC})_2(\mu_4\text{-C}_2\text{O}_4)(\text{H}_2\text{O})_3]\cdot 4\text{H}_2\text{O}$	$9.6\times 10^{-5}$	100°C, 98% RH	[4]
$\{[\text{Co}_3(\text{p-CPhHIDC})_2(\text{bpe})(\text{H}_2\text{O})]\cdot 3\text{H}_2\text{O}\}_n$	$7.04\times 10^{-4}$	100°C, 98% RH	[5]
$[(\text{Cu}^{\text{I}}_4\text{Cu}^{\text{II}}_4\text{L}_4)\cdot 3\text{H}_2\text{O}]_n$	$4.9\times 10^{-4}$	100°C, 98% RH	[6]
$\{\text{Cd}(\text{1,2,4,5-BTA})_{0.5}\}_n$	$1.0\times 10^{-4}$	100°C, 98% RH	[7]
$\{[\text{Cd}(\text{p-TIPhH}_2\text{IDC})_2]\cdot \text{H}_2\text{O}\}_n$	$1.09\times 10^{-4}$	100°C, 98% RH	[8]
$[\text{Gd}_2(\eta^2\text{-H}_2\text{L})_2(\text{H}_2\text{L})_2(\text{Phen})_2(\text{NO}_3)_2(\text{CH}_3\text{OH})]$	$8.7\times 10^{-5}$	100°C, 98% RH	[9]
$\{[\text{Sr}(\text{o-CPhH}_2\text{IDC})(\text{H}_2\text{O})_2]\cdot 2\text{H}_2\text{O}\}_n$	$6.08\times 10^{-5}$	100°C, 98% RH	[10]
<b>Compound 1</b>	$4.08\times 10^{-3}$	100°C, 98% RH	<b>This work</b>
<b>Compound 2</b>	$7.0\times 10^{-4}$	100°C, 98% RH	<b>This work</b>

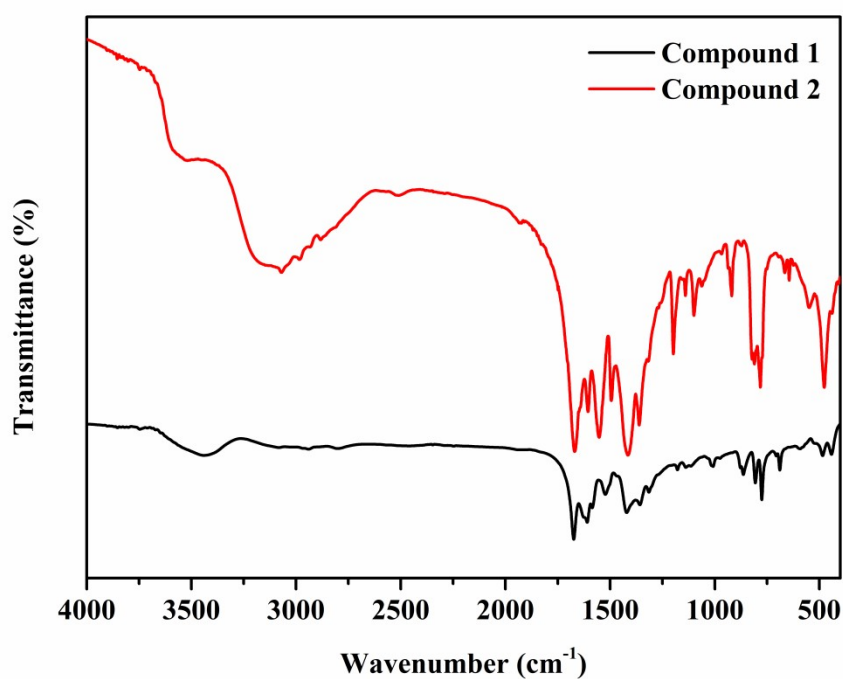


Fig.S1 Infrared spectra of compounds 1-2

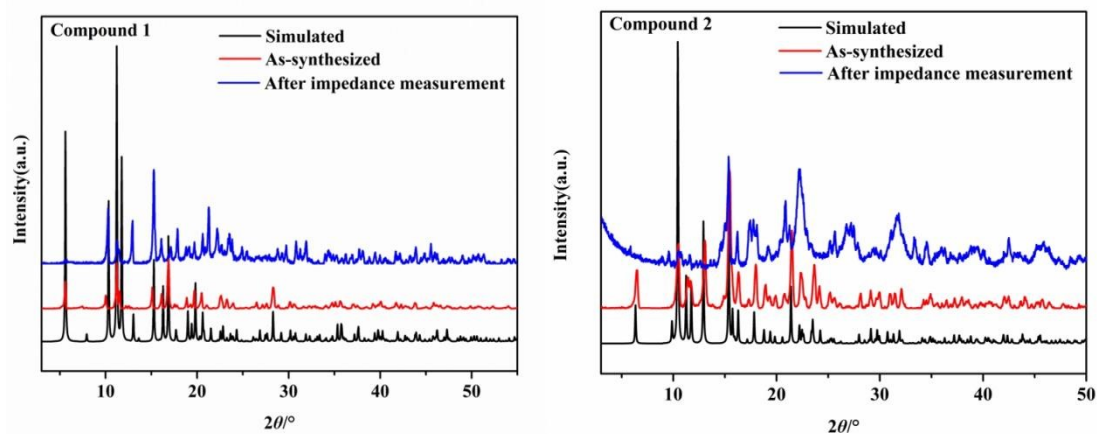


Fig. S2 PXRD patterns of compounds 1-2 samples before and after AC impedance test at 98%RH

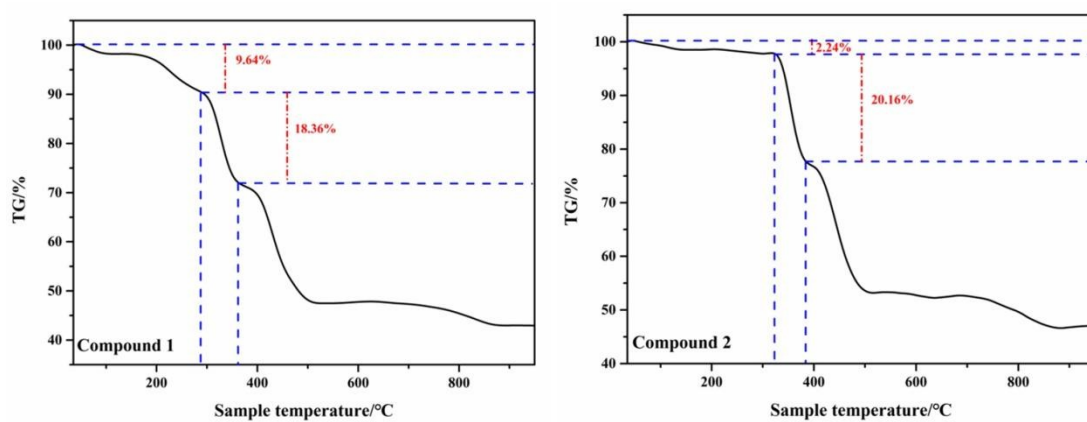


Fig. S3 TGA Curve of compounds 1-2

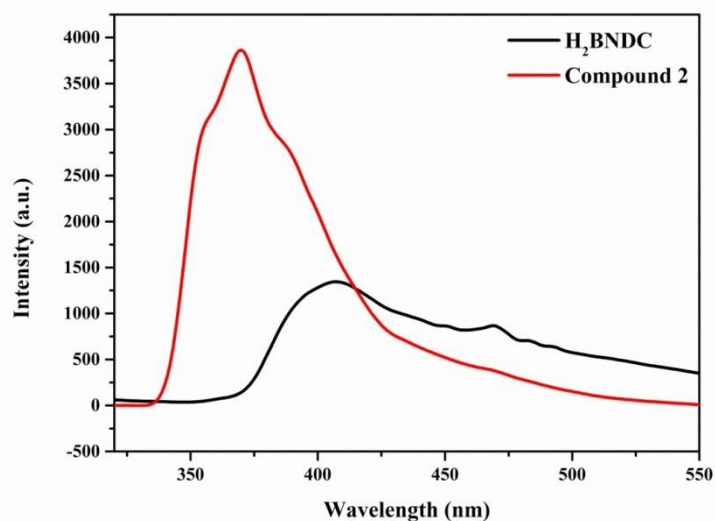


Fig. S4 Emission spectra of 2 and free ligands in solid state at 298 K

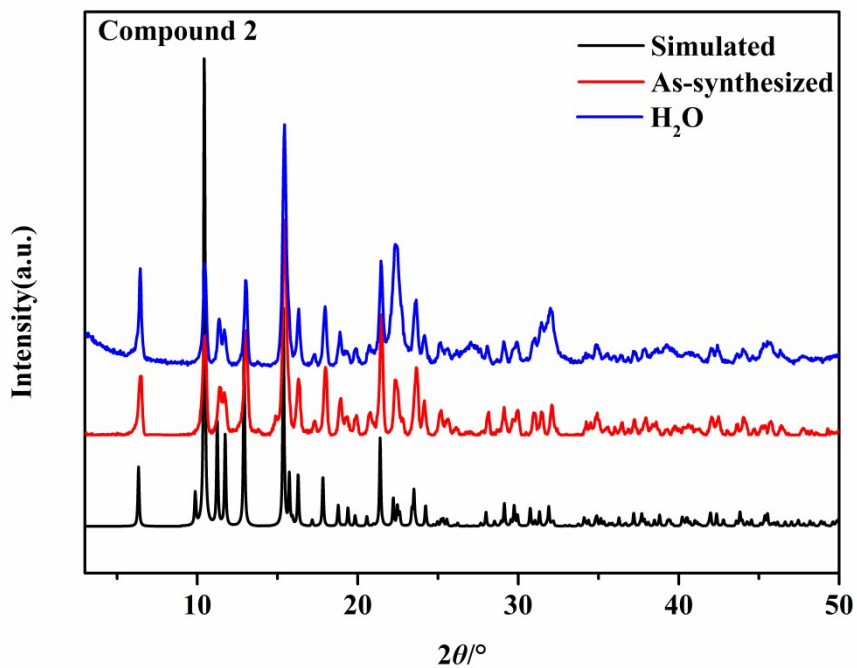


Fig. S5 PXRD patterns of compounds 1-2 immersed 24 h in H<sub>2</sub>O

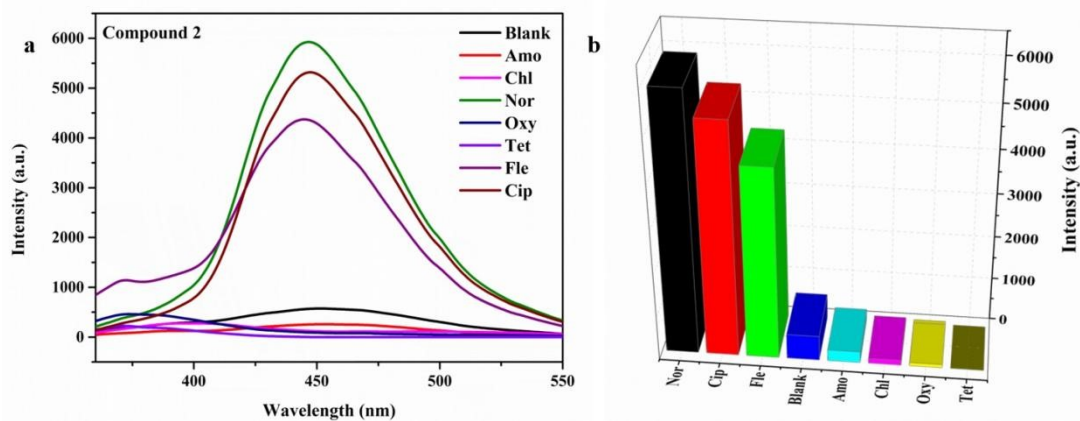


Fig. S6 (a) The photoluminescence spectra and intensities; (b) for **2** in aqueous solution with various antibiotic

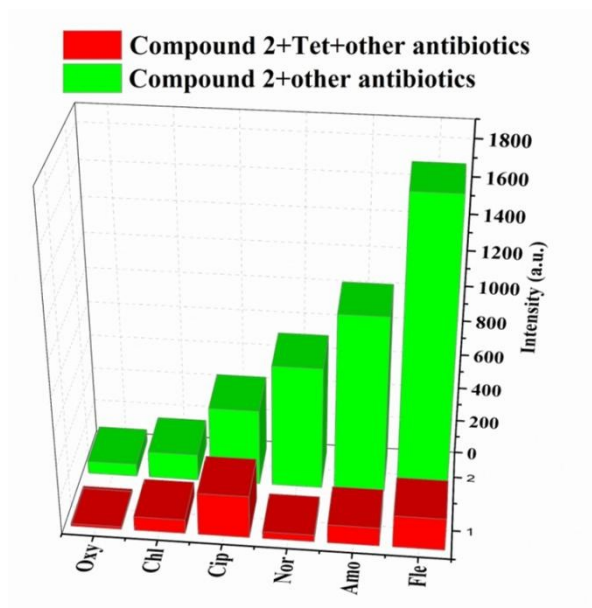


Fig. S7 Selective recognition of Tet by Compound 2 when different antibiotics coexist with Tet

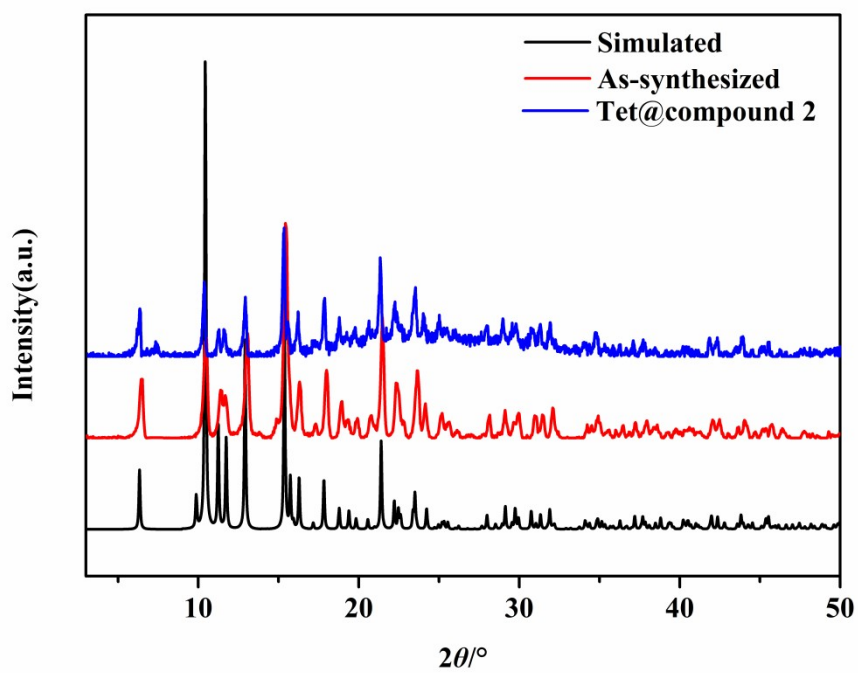


Fig. S8 PXRD patterns of compound 2 before and after sensing experiments

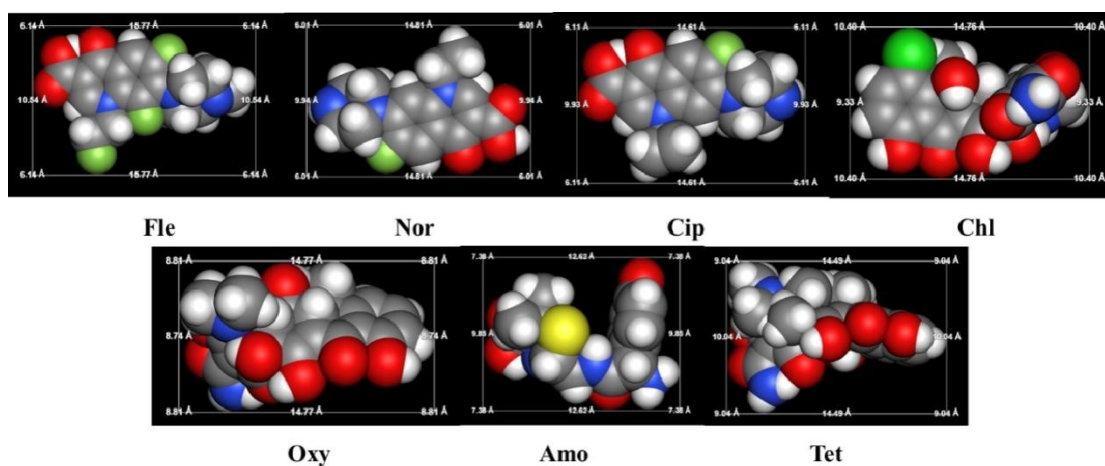


Fig. S9 Molecular size of the antibiotics

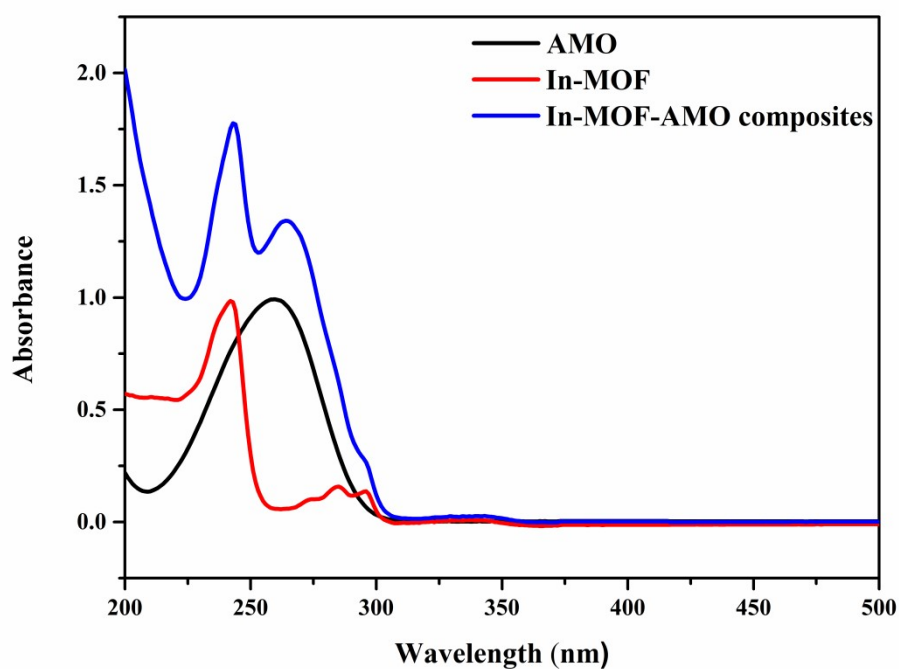


Fig. S10 UV-vis absorption of In-MOF, AMO, and composites, respectively

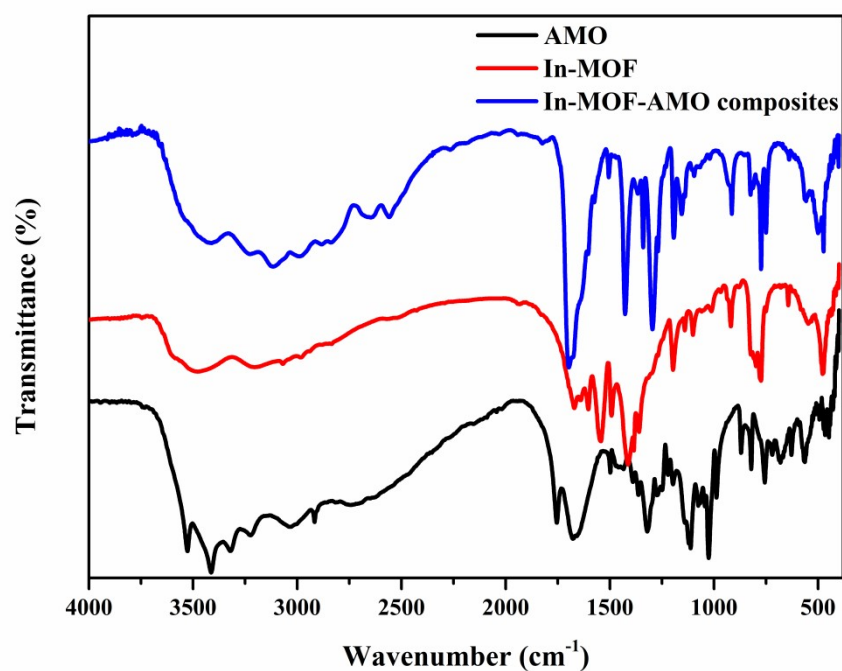


Fig. S11 Infrared spectra of In-MOF, AMO, and composites, respectively

## References

- [1] Bi Y, Wang X T, Liao W, et al. *Journal of the American Chemical Society*, **2009**, 131(33), 11650-11651.
- [2] Dolomanov O V, Cordes D B, Champness N R, et al. *Chemical Communications*, **2004** (6), 642-643.
- [3] Xie L -X, Ye Z -J, Zhang X -D, Li G. *Journal of Solid State Chemistry* **2022**, 311, 123154.
- [4] Liu R, Yu Y H, Wang H W, et al. *Inorg Chem*, **2021**, 60, 10808-18.
- [5] Liu R-L, Shi Z -Q, Wang X -Y, Li Z -F, Li G. *Chemistry – A European Journal* **2019**, 25, (62), 14108-14116.
- [6] Liu R, Zhao L, Yu S, et al. *Inorg Chem*, **2018**, 57, 11560-8.
- [7] Shi G Q, Wang H W, Wang Q X, et al. *Journal of Solid State Chemistry*, **2022**, 307, 122874.
- [8] Xie X, Zhang Z, Zhang J, et al. *Inorganic Chemistry*, **2019**, 58(8), 5173-5182.
- [9] Mu C Y, Tao Z X, Wang H W, et al. *New Journal of Chemistry*, **2021**, 45(27), 12213-12218.
- [10] Feng J, Yu S, Guo K, et al. *Polyhedron*, **2019**, 169, 1-7.